Rare Metal Materials and Engineering
Volume 50, Issue 3, March 2021
Available online at www.rmme.ac.cn

Science Press

Cite this article as: Rare Metal Materials and Engineering, 2021, 50(3): 0775-0786.

ARTICLE

Research Progress of Relationship Between Multi-scale Second Phase Particles and Properties of Al-Zn-Mg-Cu Alloys

Peng Guosheng[1], Gu Yicheng[1], Chen Songyi[2], Chen Kanghua[2], Fang Huachan[3], Song Guangsheng[1]

[1] Key Laboratory of Green Manufacturing and Surface Technology of Advanced Metal Materials, Ministry of Education, School of Materials Science and Engineering, Anhui University of Technology, Maanshan 243002, China; [2] State Key Laboratory of High Performance Complex Manufacturing, Central South University, Changsha 410083, China; [3] State Key Laboratory of Powder Metallurgy, Central South University, Changsha 410083, China

Abstract: The relationship between multi-scale second phase particles and properties of Al-Zn-Mg-Cu alloys was reviewed by related literatures and works. Multi-scale second phase particles contain micro-scale intermetallic particles, submicro-scale dispersoid, nano-scale intergranular precipitates and nano-scale intragranular precipitates. The related properties mainly refer to strength, fracture toughness and corrosion resistance. It is concluded that in Al-Zn-Mg-Cu alloys, the intermetallic particles dominate the fracture toughness and corrosion resistance, the dispersoid dominates the strength, fracture toughness and corrosion resistance via inhibiting the recrystallization of matrix, the intergranular precipitates dominate the fracture toughness and corrosion resistance, whereas the intragranular precipitates dominate the strength and fracture toughness. Furthermore, the development of techniques to manipulate multi-scale second phase was reviewed. So the possible causes and feasible technologies to synergistically improve the properties of Al-Zn-Mg-Cu alloys were pointed out, which is of great guiding significance.

Key words: Al-Zn-Mg-Cu alloys; intermetallic; dispersoid; precipitates; properties

Al-Zn-Mg-Cu age-hardening alloys with high strength and low density are widely used in aerospace field[1]. The industrial production of the Al-Zn-Mg-Cu alloys involves a series of processes (casting, homogenization, preheating, deformation, solution, quenching and aging). Every process, in essence, is related to the evolution of the second phase particles with different size scales including micro-scale intermetallic particles, submicro-scale dispersoid and nano-scale intergranular/intragranular precipitates. For example, the intermetallic particles form during the casting process, break through deformation and partly dissolve through the homogenization/solution treatment. The dispersoid and precipitate phases are precipitated from the matrix during the homogenization and aging treatment, respectively. As a result, the variation of the second phase particles has a significant effect on the properties of Al-Zn-Mg-Cu alloy. By controlling the dissolution and precipitation of multi-scale second phase particles, the properties of Al-Zn-Mg-Cu alloys are designed to meet different needs. In this research, the properties of Al-Zn-Mg-Cu alloys mainly refer to strength, fracture toughness and corrosion properties which includes pitting corrosion (PC), intergranular corrosion (IGC), exfoliation corrosion (EC) and stress corrosion crack (SCC). By reviewing the literatures and works, the relationship between multi-scale second phase particles and properties was built and the related techniques of manipulating the multi-scale

Received date: April 04, 2020
Foundation item: Anhui Provincial Natural Science Foundation (1808085ME123); International Cooperation and Exchanges in Anhui Provincial Key Project of Research and Development Plan (1804b06020363)
Corresponding author: Peng Guosheng, Ph. D., Associated Professor, School of Materials Science and Engineering, Anhui University of Technology, Maanshan 243002, P. R. China, Tel: 0086-555-2311570, E-mail: pengguosheng@126.com

particles to improve the properties were summarized in the view of the composition and heat treatment.

1 Micro-scale Intermetallic Particles

1.1 Type and formation of micro-scale intermetallic particles

Intermetallic particles always exist in the microstructure of 7000 series Al alloys. Typically, the intermetallic particles occupy a little volume in the wrought microstructure, and generally grow up to micrometer scale in size[2]. Intermetallic particles consist of the soluble intermetallic particles, such as Al_2CuMg (S), $Al_2Mg_3Zn_3$ (T) and $MgZn_2$ (η) phases, and insoluble intermetallic particles, such as Al_7Cu_2Fe phases (Fig.1)[3]. The soluble intermetallic particles form from the last-freezing liquid as a consequence of the micro-segregation at the stage of solidification and can redissolve into the solution during the subsequent heat treatment[4]. Insoluble intermetallic particles often contain Fe/Si contaminants due to the presence of Fe/Si as a natural impurity and their extremely low solid solubility at room temperature[5]. Insoluble intermetallic particles only change in morphology, crystal type and composition through deformation and heat treatment. All coarse intermetallic particles mainly form during the direct-chill ingot-casting process, which is a prevailing casting process for 7000 series Al alloys.

1.2 Effect of micro-scale intermetallic particles

In a common sense, intermetallic particles are deleterious to the properties of Al-Zn-Mg-Cu alloy, especially for the fracture toughness and corrosion resistance (particularly pitting corrosion). The formation of intermetallic particles not only decreases the aging-hardening effect due to the loss of the alloy element, but also increases the origins of fracture/corrosion. It is well accepted that the first step in the process of fracture is the nucleation, growth and coalescence of voids in intermetallic particles (Fig.2)[6]. Based on the relationship between the fracture toughness and intermetallic particles, the model is successfully built, where the fracture toughness (K_{IC}) is proportional to $f_c^{-1/6}$ (f_c is the volume fraction of intermetallic particles)[7]. The fracture associated with the intermetallic particles shows large and

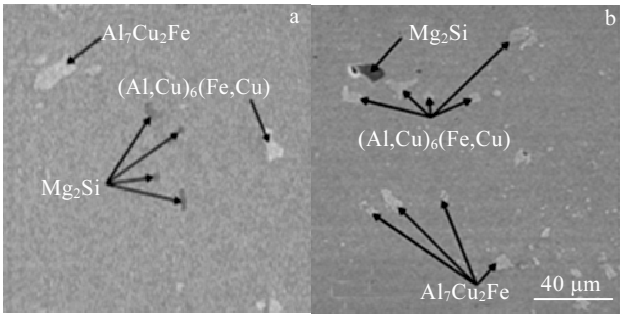

Fig.1 Intermetallic in AA7075 after T6 treatment (a) and solution heat treatment (b)[3]

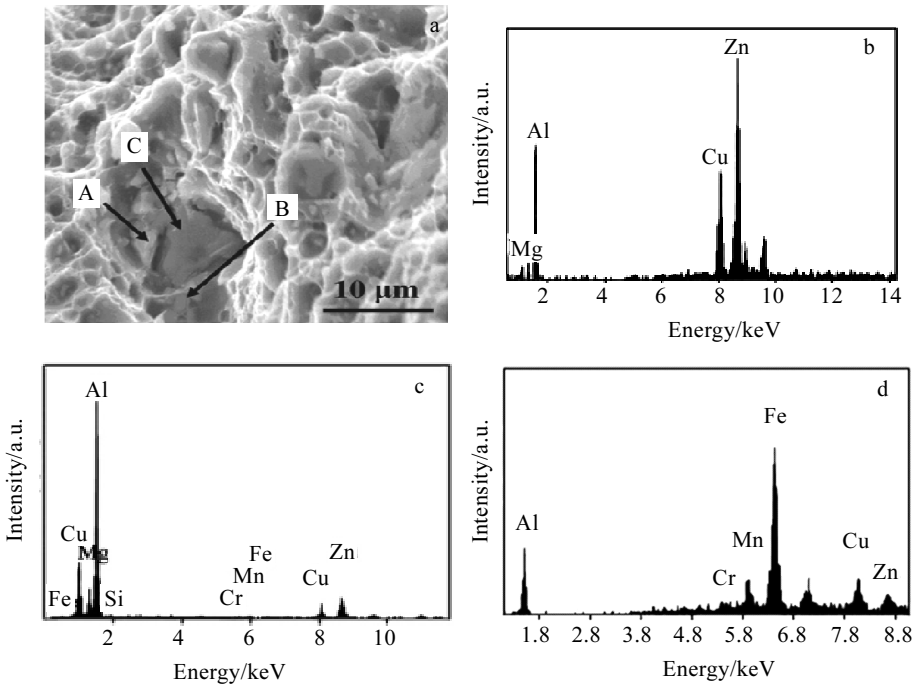

Fig.2 SEM morphology of broken specimen (a) and EDS analyses of points in Fig.2a (b~d): (b) point A, η-$Mg(Zn,Cu,Al)_2$; (c) point B, S-$CuMgAl_2$; (d) point C, $(Cu, Fe, Mn)Al_2$[6]

shallow dimples, in the center of which lies the cracked intermetallic particles. The insoluble (Fe, Si)-rich intermetallic particles are more detrimental to the fracture toughness than the soluble intermetallic particles since they cannot dissolve into the matrix by heat treatment. Cvijović et al[6] found that with increasing the volume fraction of (Fe, Si)-rich intermetallic particles from 0.352vol% to 0.737vol%, the corresponding fracture toughness decreases from 43.2 MPa·$m^{1/2}$ to 37.7 MPa·$m^{1/2}$. As a comparison, the strength keeps the same, even slightly increases. They claimed that the strength is not very sensitive to intermetallic particles. Since the intermetallic particles easily lead to the concentration of stress (or dislocations) during the deformation process, they accelerate the occurrence of recrystallization at the following stage of solution. The recrystallization is harmful to the strength of Al-Zn-Mg-Cu alloy. As a result, intermetallic particles have an indirect harmful effect on the strength of Al-Zn-Mg-Cu alloys. In addition, the intermetallic particles, due to different corrosion potentials with α-Al, often induce pitting corrosion (Fig.3)[8]. Birbilis et al[9] summarized the corrosion potentials of intermetallic particles commonly existing in Al alloys with high strength in 0.1 mol/L NaCl solution via the micro-capillary electrochemical cell, as shown in Table 1. It can be seen that compared with the corrosion potential of α-Al, the corrosion potentials of Al_3Fe, Al_2Cu, Al_7Cu_2Fe and Al_2CuMg phases are more positive, indicating that α-Al near these phases dissolves first and leads to the detachment of intermetallic particles. Similarly, the corrosion potentials of $MgZn_2$ and Mg_2Si are more negative than those of α-Al, resulting in the total or part dissolution of intermetallic particles[10]. Since the stress corrosion crack is due to the fracture behavior in corrosion environment, the role of intermetallic particles in SCC is related to the synergistic effect of both the corrosion resistance and fracture toughness[11], which means that the intermetallic particles are also detrimental to SCC, acting as the origin of corrosion and crack[12,13], as shown in Fig.4.

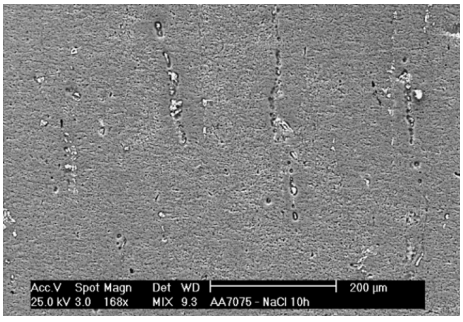

Fig.3 SEM image of pitting corrosion nearby the Al_7Cu_2Fe of 7075-T651 immersing in 0.1 mol/L NaCl solution for 10 h[8]

Table 1 Electrochemical data for intermetallic particles at pH=6[9]

Composition	Phase	Corrosion potentials/mV vs. SCE
Al_3Fe	β	−539
Al_2Cu	θ	−665
$MgZn_2$	η	−1003
Mg_2Si	β	−1538
Al_7Cu_2Fe	-	−551
Al_2CuMg	S	−883
α-Al	-	−900

Note: the corrosion potential of most Al-Zn-Mg based alloys is nominally about −900 mV in the neutral NaCl solution[9]

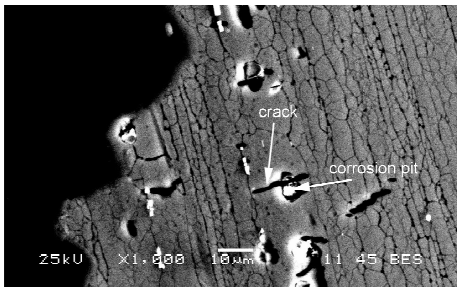

Fig.4 SEM image of the slow strain rate test (SSRT) sample etched by Graff Sargent's reagent[12]

1.3 Techniques development of intermetallic for decreasing the detrimental effect

To improve the fracture toughness and corrosion resistance of Al-Zn-Mg-Cu alloys, it is necessary to minimize the volume fraction of intermetallic particles in the final products. For soluble intermetallic particles, the techniques to decrease the volume fraction include the optimization of alloy composition[14-16] and enhancing heat treatment[17-19]. For example, in 7449 alloy, the suppression of S phase is achieved by decreasing the copper content, which is relative to the copper content of the 7150 alloy[14]. Similarly, the residual eutectic phase decreases when Cu content decreases to 2.2wt% in Al-9.3Zn-2.4Mg-*x*Cu-Zr alloys after homogenization[15]. In addition, the amount of coarse T (AlZnMgCu) phases decreases with the decrease of Zn content in high Zn-bearing Al-Zn-Mg-Cu alloys[16]. Besides, the enhancing heat treatment is mainly applied to the stage of homogenization or solution treatment. The basic steps for the enhancing heat treatment, namely enhanced solution treatment or multi-steps homogenization, are as follows: (1) the sample is held at low temperature for a certain time to ensure the dissolution of eutectic phase; (2) gradually increasing the temperature to maximize the dissolution of soluble intermetallic particles. The multi-staged heat treatment can avoid overheating of the eutectic phase with low

melting point. For example, Song et al[17] reported that the multi-staged solution treatment can improve the dissolution of the second phase particles and concurrently minimize the occurrence of recrystallization within the range of solution temperature. Gao[18] and Peng[19] et al obtained the similar conclusions by multi-step homogenization.

The insoluble intermetallic particles of Al-Zn-Mg-Cu alloy, mainly refers to Fe/Si-rich phases, show a more detrimental effect on the fracture and corrosion behavior. In order to minimize the detrimental influence of insoluble intermetallic, the raw materials with high purity are used. It is a developing trend for 7000 series Al alloys with high fracture toughness and corrosion resistance to decrease the content of Fe/Si impurity. However, it unavoidably increases the cost of materials and possibly brings some new problems, such as mould soldering[20] and crack sensitivity[21]. Considering the mentioned factors, the Al-Zn-Mg-Cu alloys contain some Fe/Si impurities due to the technical problem of Al electrolysis or the use of recycled raw materials. Hitherto, there are two practical approaches to reduce the detrimental effect of intermetallic particles containing Fe/Si impurity[22]. When the content of Fe/Si element is high, Fe/Si impurity can be scavenged via the settling-down method by the reaction of Fe/Si element and other elements forming Fe/Si-rich compounds[23]. For alloys with low content of Fe/Si element, the refinement of Fe/Si-rich phases via enhancing heterogeneous nucleation or the modification of Fe/Si-rich phases by adding minor elements is effective[24,25]. In addition, the increasing solidification rate of Al alloy[26] or the increasing amount of deformation[27] to break fragile Fe/Si-rich phases can also refine the Fe/Si-rich phases when the processing condition is suitable.

2 Submicro-scale Dispersoid

2.1 Type and formation of submicro-scale dispersoid

The commercial well-known submicro-scale dispersoid is $Al_{12}Mg_2Cr$ (E), $Al_{20}Mn_3Cu_2$ and Al_3Zr phases in Al-Zn-Mg-Cu alloys. Before the solidification casting, Cr, Mn or Zr elements easily form a supersaturated Al-based solid solution due to their low diffusivity. When the alloys are held at the homogenization temperature, the Cr, Mn or Zr elements are precipitated from the solidified Al matrix in the form of spherical dispersoid with a diameter of 10~20 nm due to the decrease of solubility with temperature. Since the major role of dispersoid is to inhibit the subsequent recrystallization, the effect of dispersoid on the properties is attributed to the recrystallization in Al-Zn-Mg-Cu alloy[28].

2.2 Effect of recrystallization

It is well documented that the recrystallization has an adverse effect on the strength[29], fracture toughness[30] and corrosion properties[31,32]. Since the recrystallization is associated with the migration of grain boundary, the corrosion properties predominated by the recrystallization mainly refer to IGC, EC and SCC, which occur at the grain boundary. As Dorward et al[29] reported, the recrystallization significantly decreases the strength and fracture toughness and increases the quench sensitivity (Fig.5), due to the possible mechanism that a coherent crystallographic orientation of Al_3Zr becomes incoherent with the occurrence of recrystallization, thereby acting as effective nuclei for $MgZn_2$ precipitation during the quench. Transmission electron microscope (TEM) observations support the mechanism (Fig.6)[33]. Therefore, the coarse $MgZn_2$ precipitates on the incoherent Al_3Zr particles deplete the solute in the matrix and form the precipitate free zone (PFZ) during the quench, which is deleterious to age-hardening and fracture toughness. The corresponding fracture mode is coarse voiding. The recrystallization also degrades the IGC, EC and SCC resistance. It is known that EC initiated from IGC and SCC exclusively results in intergranular fracture in Al-Zn-Mg-Cu alloys. Therefore, three types of corrosion forms (IGC, EC, SCC) depend on the intergranular precipitates, which reply on the grain structure[34,35]. The phenomena are also found in other alloy systems[36-38]. For example, Minoda[36] observed that IGC mainly occurs at the high angle grain boundaries in 6000 series Al alloys (Fig.7). Compared with the unrecrystallized grain boundary, the recrystallized grain boundary consists of more grain boundaries with high angle and endures higher grain boundary energy (Fig.8)[39]. Therefore, the intergranular precipitates nucleate more readily and grow at the recrystallized grain boundary, resulting in the coarser intergranular precipitates and wider PFZ (Fig.9). The microstructural features at the recrystallized grain boundary are deleterious to the fracture toughness and corrosion resistance, compared with those at the unrecrystallized grain boundary. The corresponding fracture mode associated with the intergranular precipitates is the intergranular fracture along the high-angle grain boundaries.

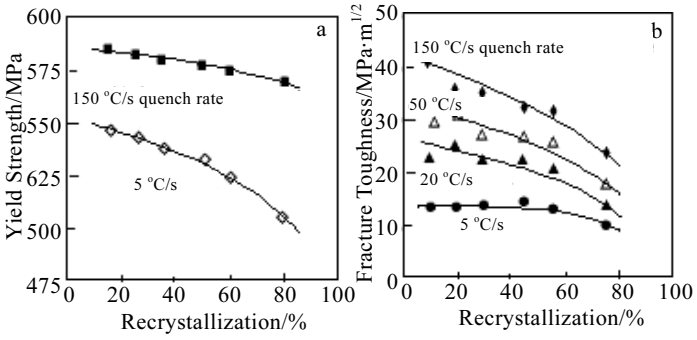

Fig.5 Effect of recrystallization and quench rate on the yield strength (a) and fracture toughness (b)[29]

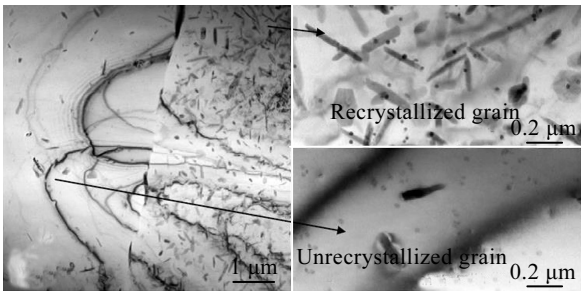

Fig.6 Typical TEM microstructures of AA7050 after low rate quenching and solution[33]

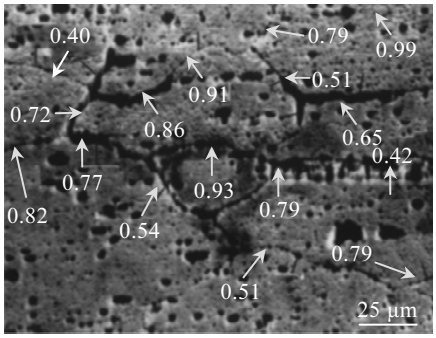

Fig.7 OM image of cross section of sample after IGC test (the numbers indicate the misorientation angle of the corroded boundaries, rad)[36]

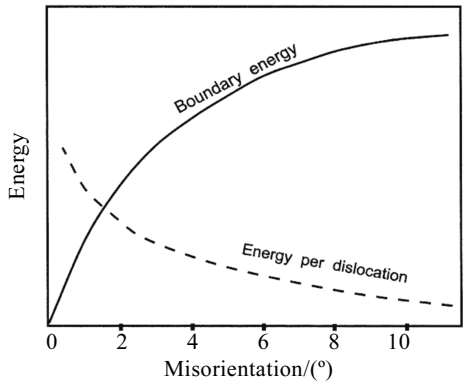

Fig.8 Relationship between grain boundary energy and grain boundary misorientation angle[39]

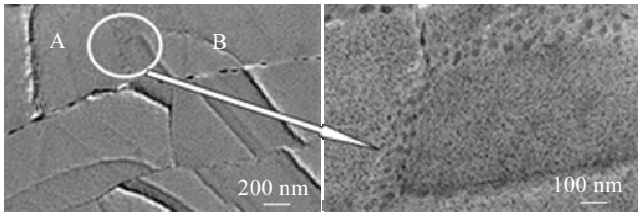

Fig.9 Intergranular precipitation behavior at different grain boundaries (A denotes the unrecrystallized grain boundary; B denotes the recrystallized grain boundary)

2.3 Development of techniques for dispersoid inhibiting recrystallization

To inhibit the recrystallization of Al matrix more effectively, the development of new dispersoid, optimizing homogenization, deformation and solution treatment is adopted. The introduction of small quantities of Cr or Mn improves the resistance to recrystallization, but the dispersoid containing Cr or Mn is sensitive to quench, due to the fact that $MgZn_2$ (η) phase is precipitated on the incoherent interface of $Al_{12}Mg_2Cr/Al_{20}Mn_3Cu_2$ dispersoid[40]. This leads to the loss of aging-hardening and the crack origin. Zr addition forms the coherent $L1_2$ structure of Al_3Zr dispersoid, which is considered to be not as quench-sensitive as $Al_{12}Mg_2Cr/Al_{20}Mn_3Cu_2$ dispersoid (Fig.10)[33]. It attributes to the difficulty of nucleating η phase on the coherent Al_3Zr dispersoid, resulting in higher strength and fracture toughness. Therefore, it leads to the replacement of Cr-containing 7X75 alloys by Zr-containing 7X5X alloys. Recently, it was also observed that Zn and Cu elements are segregated on Al_3Zr dispersoid, suggesting that it may have a secondary effect in promoting heterogeneous nucleation for undesirable quench-induced precipitation (Fig.11)[41]. Al_3Zr dispersoid is thermodynamically metastable and transforms to its equilibrium structure D023 above 475 °C[42], which restricts the application of Al_3Zr at high temperature. Although Al_3Sc dispersoid has a thermodynamically stable $L1_2$ structure, it easily coarsens above 300 °C because Sc element has a relatively large diffusivity in aluminum[43]. The features discourage the stability of Al_3Sc at high temperature. Adding Zr to Al-Sc alloys is a good strategy to utilize the merits of both Zr and Sc elements. The formation of $Al_3(Sc, Zr)$ with $L1_2$ structure improves the stability and coarsening resistance at 300 °C, compared with Al_3Zr or Al_3Sc[44-46]. $Al_3(Sc, Zr)$ dispersoid exhibits a typical core/shell structure with Sc-rich core and Zr-rich shell. Owing to the faster diffusivity of Sc (compared with that of Zr) in the solid solution, the Sc-rich core forms at the initial stage and improves the nucleating rate of dispersoid, leading to more dispersoid precipitation. For the same reason, the Zr-rich shell forms at the later stage, which decreases the coarsening rate of dispersoid. Both factors make the $Al_3(Sc, Zr)$ dispersoid more stable with stronger coarsening resistance[44]. Robson[45] predicted that adding Sc into Zr-containing 7050 alloys can improve the distribution of dispersoid and significantly enhance the recrystallization resistance. Zhang et al[46] claimed that the mechanical properties of Al-Zn-Mg-Cu alloy improve greatly by adding Zr and Sc (UTS=747 MPa, YS=721 MPa and EI=10.9%). The addition contributes to the grain refinement by the primary $Al_3(Sc, Zr)$ and the dispersion strengthening of the secondary $Al_3(Sc, Zr)$. Many researches focused on other transition elements[47,48] or rare earth (RE) elements to substitute Sc/Zr[49-52] to improve thermal stability and recrystallization inhibition ability. The alloy partly substitutes rare

earth elements, including Yb[49] and Er[52], for Sc forming Al_3(Sc, RE) with $L1_2$ structure, which has a larger lattice parameter mismatch with aluminum, thereby enhancing the elastic interactions with dislocations and improving the creep resistance of the alloy. In our studies, Al_3(Zr, Yb) dispersoid forms when Al_3Yb dispersoid incorporates Zr, exhibiting a unique core/shell structure and a better thermal stability and recrystallization inhibition ability, compared to the effect of Al_3Zr in pure aluminum (Fig.12)[49].

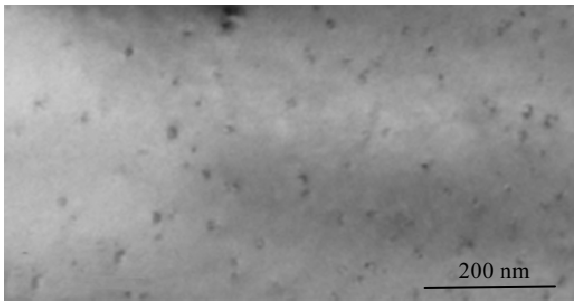

Fig.10 TEM image of Al_3Zr dispersoid in the homogenized 7055-0.15Zr alloy[33]

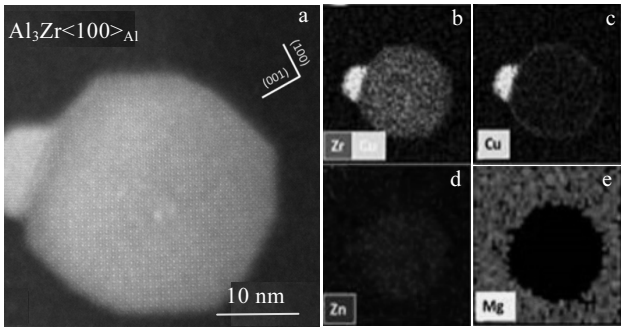

Fig.11 Al_3Zr dispersoid particle with a barnacle-like precipitate: (a) STEM-HAADF image and (b~e) element mapping analysis results[41]

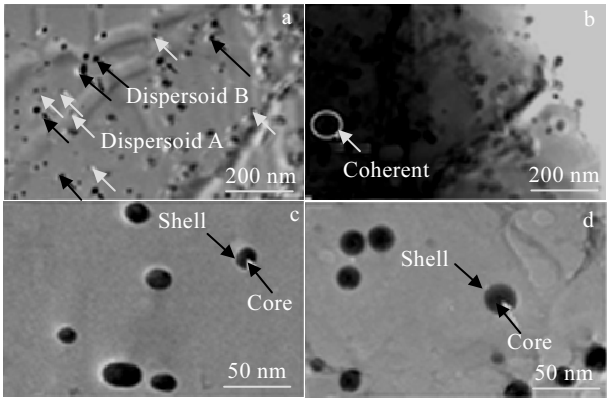

Fig.12 TEM bright field image of dispersoid (a) and detailed images of dispersoid A (b) and dispersoid B (c, d) in Fig.12a of as-homogenized Al-0.9Zr-1.73Yb alloys[49]

Due to the Zr segregation during the casting, the distribution of Al_3Zr precipitates is not uniform, especially at the edges of dendrites, where insufficient Al_3Zr precipitates are observed[53]. Traditional one-step homogenization cannot obtain dispersoid with high number density and homogeneous distribution, because low homogenization temperature restricts the diffusion rate of Zr element, whereas high homogenization temperature increases the solubility of Zr element. Based on the facts, multi-step homogenization was developed to obtain favorable Al_3Zr distribution[54,55]. The basic principle for multi-step homogenization is to encourage dispersoid nucleation at the initial low temperature homogenization before the final high temperature homogenization. Both two-step homogenization proposed by Robson[54] and three-step homogenization proposed by Deng[55] showed that the multi-step homogenization can improve the uniform distribution of Al_3Zr dispersoid, resulting in the decrease of recrystallization during hot-rolling and solution heat treatment. In addition, optimizing deformation[56] or solution condition[57] was performed to keep the maximum ability of dispersoid for inhibiting the recrystallization of Al matrix.

3 Nano-scale Intergranular Precipitates

3.1 Type and formation of nano-scale intergranular precipitates

In Al-Zn-Mg-Cu alloys, intergranular precipitates are mainly $MgZn_2$ or compounds containing Cu/Al element with a certain concentration. Since the grain boundary belongs to plane defects with higher energies, the precipitation behavior of intergranular precipitates is thermodynamically faster than that of intragranular precipitates. Therefore, the intergranular precipitates are initially precipitated during the quench treatment, and then develop during the following aging treatment, whereas the intragranular precipitates are only precipitated during the aging treatment. It means that the intergranular precipitates of 10~40 nm are coarser than the intragranular precipitates of 3~10 nm. The precipitation behavior of intergranular precipitates, therefore, depends on the quenching and aging treatment. In addition, the PFZ forms through the intergranular precipitation, with 50~150 nm in width. The PFZ formation may be due to two different mechanisms: (1) the vacancy-depleted PFZ, where vacancies disappear at the grain boundary; (2) the solute-depleted PFZ, where normal nucleation and growth of the equilibrium phase occur at the grain boundary, depleting the solute in adjacent regions, and producing a solute-depleted PFZ.

3.2 Effect of nano-scale intergranular precipitates

The effect of intergranular precipitates on the properties mainly refer to the fracture toughness (intergranular fracture) and corrosion (IGC, EC and SCC) at the grain boundaries. The microstructural features of intergranular precipitates include the morphology, composition and PFZ

width. The morphology of intergranular precipitates is determined by their continuity, area fraction and size. Discontinuous intergranular precipitates are beneficial to the fracture toughness and the corrosion resistance because they cut the route of fracture and corrosion (IGC, EC and SCC) crack. Discontinuous intergranular precipitates are typical features for over-aging alloys. Over-aging treatment can improve the fracture toughness and corrosion resistance of alloys compared with peak-aging treatment[58]. With the development of discontinuity, the intergranular precipitates are gradually coarser. The coarse intergranular precipitates are also good for the fracture toughness and corrosion resistance compared with the small intergranular precipitates after peak-aging treatment. According to the hydrogen embrittlement theory, the coarse intergranular precipitates readily act as the trapper for H atoms and reduce the concentration of atomic hydrogen at the grain boundaries, which improves SCC resistance. However, the excessive coarse intergranular precipitates readily become a resource of fracture and correspond to the fracture mode of intergranular fracture. When alloys are treated with low quenching rate, the excessive coarse intergranular precipitates are precipitated during the quenching and aging process. It significantly degrades the strength and fracture toughness[33]. Similarly, the excessive coarse intergranular precipitates may lead to the anodic dissolution, resulting in the poor corrosion resistance[59]. Besides, the composition of intergranular precipitates has a significant effect on corrosion (IGC, EC, and SCC) resistance[60]. It is also known that the ideal intergranular precipitates for 7000 series alloys are $MgZn_2$ phases and their corrosion potential is negative relative to that of α-Al, indicating that the $MgZn_2$ phases preferentially dissolve in corrosive environment. It degrades the corrosion resistance of Al-Zn-Mg-Cu alloys. As a comparison, the increasing Cu content in $MgZn_2$ increases the corrosion potential of $MgZn_2$ and decreases the potential difference between $MgZn_2$ and α-Mg, resulting in the improvement of corrosion resistance of alloys due to the weakening effect of galvanic cell. In addition, the segregation of element Mg at the grain boundaries accelerates the formation of stress corrosion cracks by the increasing adsorption of atomic hydrogen and diffusion[61]. PFZ usually has a deleterious effect on the fracture toughness and corrosion (IGC, EC and SCC) resistance. Since PFZ is free of precipitates, it is softer than the surrounding matrix, and under an applied stress, it can be the region of strain localization. This may lead to the premature fracture and degrade the fracture toughness of alloys. In addition, PFZ can decrease the SCC resistance since it leads to the failure of both mechanically and environmentally induced fractures.

3.3 Development of techniques to manipulate intergranular precipitates

In Al-Zn-Mg-Cu alloys, the relative coarse and discontinued Cu-rich intergranular precipitates combined with narrow PFZ are ideal microstructural features, which are manipulated by the optimization of composition and heat treatment. It is well acknowledged that the principle to determine appropriate Cu content in 7000 series Al alloys is that no excess Cu-containing intermetallic particles form after Cu alloy incorporates into the intergranular precipitates, which results in the improvement of corrosion resistance without the loss of fracture toughness of alloys. Marlaud et al[62] found that Cu content in precipitates increases with increasing the Cu alloy content in Al-Zn-Mg-Cu alloys.

Since the intergranular precipitates nucleate and grow during the quenching and aging process, their status depends on the quench and aging process. The vacancies induced by quenching play critical roles in the solute atom segregation at the grain boundary[63,64]. The quenching rate determines the composition of intergranular precipitates and the width of PFZ. A lower quenching rate leads to a higher content of Zn, Mg and Cu in intergranular precipitates and a greater width of PFZ due to the sufficient diffusion time for solutes at high temperature, resulting in weaker exfoliation corrosion resistance[65]. Therefore, the quenching rate should be as fast as possible if the quenching techniques and residual stress deformation are allowed. Besides, the intergranular precipitates are affected by the grain structure and aging treatment. It is necessary to note that the aging treatment only modifies the features of the precipitates but does not change the grain structure. Therefore, the effect of aging treatment on the properties only relates to the precipitates and has no relationship with grain structure. Azarniya et al[66] reviewed the development of various aging treatments and their effects on the microstructure and properties. With the increase of aging extent, the intergranular precipitates become coarse and discontinuous with concomitant induced by the increase of Cu content and the decrease of Mg content (Fig.13 and Table 2[61]). The variation of intergranular precipitates via over-aging treatment is beneficial to fracture toughness and corrosion resistance of Al-Zn-Mg-Cu alloys (Fig.14)[67].

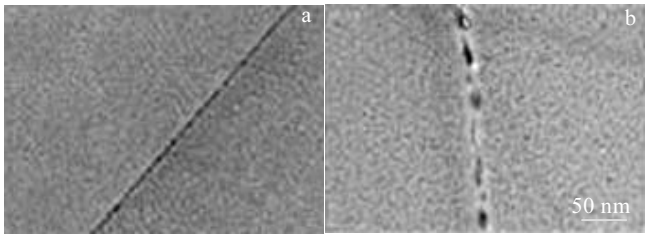

Fig.13 TEM morphologies of precipitates in 7B50 alloy at 120 °C for different time: (a) peak aging treated and (b) over-aging treated

Table 2 Mg, Zn, Cu contents of precipitations at the grain boundary after different aging treatments (at%)[61]

Aging treatment	Mg	Zn	Cu	Solid solution Mg
418 K/5 h	8.35	3.15	4.90	6.78
418 K/8 h	6.74	3.45	3.91	5.02
418 K/16 h	6.60	2.80	4.15	5.20
418 K/24 h	6.08	4.09	2.43	4.04
418 K/36 h	6.63	4.86	2.60	4.20

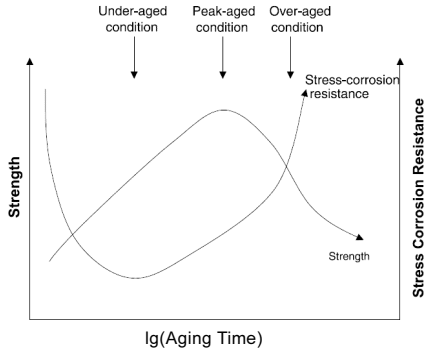

Fig.14 Effect of aging time on stress corrosion resistance and strength[67]

Over-aging treatment improves the fracture toughness and corrosion resistance with the loss of strength in some extent since the intragranular precipitates simultaneously coarsen with the coarsening of intergranular precipitates. To obtain superior comprehensive properties for 7000 series Al alloy, the microstructural features, which contain coarse and discontinuous intergranular precipitates and fine intragranular precipitates with high number density, are in need and the corresponding heat treatment techniques are developed. Retrogression and re-aging (RRA)[68] temper has been studied. The difference between RRA temper and T6 or T7 temper is that the intergranular precipitates become coarse and discrete whereas intragranular precipitates partially dissolve into the matrix during RRA process. Considering that the RRA temper is inappropriate for large and thick workpiece, the repetitious-RRA[69], multi-stage aging[70], step quench and aging (SQA) treatment[71] and slow quench rate[72] are proposed. The main feature of tempers mentioned is to avoid the uncompleted retrogression when short retrogression time is applied to the large and thick workpiece. High-temperature pre-precipitation[73,74] temper is similar to SQA temper, which increases the Cu content of intergranular precipitates due to the increasing diffusion rate for Cu atoms when the samples are held at high temperature. In addition, Wang[75] claimed that the strength and SCC of sample with severe cold rolling after solution treatment improve compared to those of sample after T6 treatment.

4 Nano-scale Intragranular Precipitates

4.1 Type and formation of nano-scale intragranular precipitates

Al-Zn-Mg-Cu alloys are heat-treatable because they respond to precipitation hardening during the aging treatment following the quenching and solution treatments. The alloying elements (Mg, Zn and Cu) have large solubility in Al matrix at high temperature and the solubility of alloying elements decreases with decreasing the temperature. Therefore, the alloying elements beyond their equilibrium solid solubility are precipitated away from the Al matrix in the form of nano-size precipitates. It is well documented that the intragranular precipitates mainly refer to Mg(Zn, Cu, Al) phase (η) and related compounds, and the general sequence of precipitation in alloys is as follows: supersaturated solid solution → Guinier-Preston (GP) zone → η'→ η.

GP zones are isomorphous with the matrix, resulting in a lower interfacial energy than intermediate or equilibrium precipitate phase has. GP zones, therefore, form firstly on the basis of the solute atom cluster at the initial aging stage. With the longer aging time, the semi-coherent η and non-coherent η' phases form in sequence to decrease the strain of precipitates in Al matrix[76].

4.2 Effect of intragranular precipitates

It is well acknowledged that the occurrence of precipitate phases in alloys depend on the quenching and aging process (Fig.15)[77]. The quenching sensitivity determines the age-hardening response of Al-Zn-Mg-Cu alloys[78]. The coarse Mg(Zn, Al, Cu) phase in alloys with high quenching sensitivity are readily precipitated on the dispersoid or at the grain boundary, which is detrimental to the strength and fracture toughness. The predominant intragranular precipitates under under-aged, peak aging and over-aging conditions are associated with the coherent GP zone, the semi-coherent η phase and the η or a mixture of η and η' phases, respectively[79]. The intragranular precipitates dominate the strength and the fracture toughness of Al-Zn-Mg-Cu alloys. The strengthening mechanism involves the interaction of dislocations with intragranular precipitates during plastic deformation. The interaction contains two cases, depending on the orientation relationship of precipitates and α-Al. One is the shearable precipitates (GP zones and η' phase), where the dislocations are able to cut through. The increase of the number density of the shearable precipitates leads to the increase of strength with aging. However, the local dislocations pile up after the dislocations cut through the precipitates and the strength difference between intra-grain and inter-grain increases, leading to the decrease of fracture toughness. The other is non-shearable precipitates (η phase). The precipitates are non-coherent with α-Al and the dislocations have to either climb or leave a dislocation loop around the precipitates,

which leads to the homogeneous deformation. The coarsening intragranular precipitates decreases the strength with aging. In addition, the strength difference between intra-grain and inter-grain decreases and the homogeneous plastic deformation improves the fracture toughness (Fig.16)[80]. The fracture mode associated with the intragranular particles is mainly ductile shear fracture and ductile intragranular fracture at under-aged status and peak or over-aging status, respectively (Fig.17 and 18)[81,82].

4.3 Development of techniques to manipulate intragranular precipitates

To maximize the number density of intragranular precipitates, alloying element optimization has been widely studied. It was reported that Cu addition in Al-Zn-Mg alloys promotes the precipitation hardening by stabilizing GP zones and retarding the early stage of decomposition. However, Cu introduction increases the quench sensitivity. Therefore, the appropriate Cu content should be designed for special application. For example, low Cu-containing 7085 Al alloys are developed to apply for the large and thick workpiece, which demands low quench sensitivity and high fracture toughness. Ag addition can also increase the strength of Al-Zn-Mg alloys with the similar strengthening mechanism as that of Cu addition[83]. Besides, the increase of Mg content or decrease of the ratio of Zn/Mg can increase the strength and quench sensitivity[84].

Besides T6, T7 and RRA temper treatments, the new tempers were developed. Jiang et al[85] found that the non-isothermal aging treatment process improves the mechanical performance and corrosion resistance for Al-Zn-Mg-Cu alloys, compared with those of alloys after

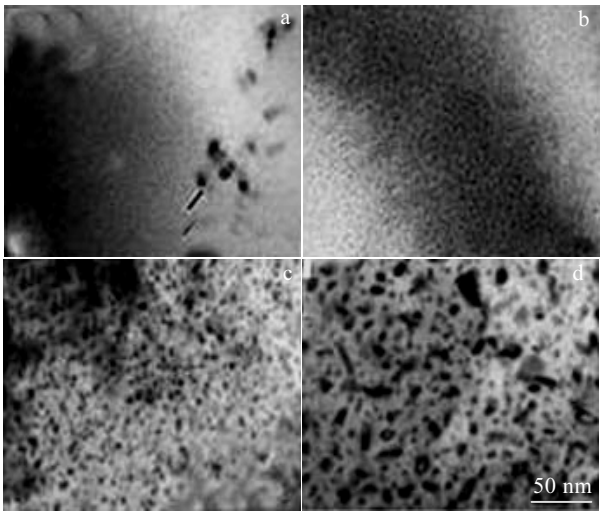

Fig.15 TEM images of precipitates in samples aged under different conditions: (a) 120 °C/2 h; (b) 120 °C/36 h; (c) 140 °C/48 h; (d) 160 °C/36 h[77]

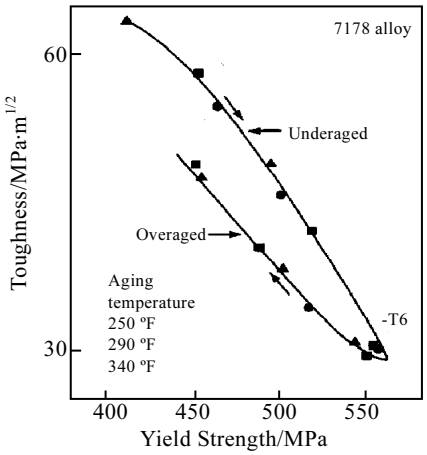

Fig.16 Effect of aging on the yield strength and toughness (arrows indicate changes with increasing the aging time)[80]

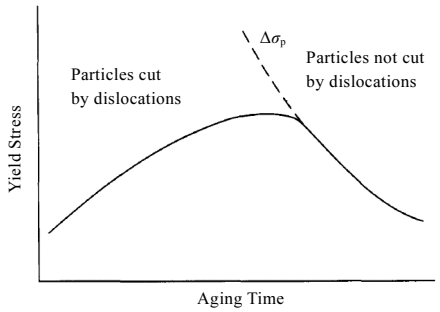

Fig.17 Schematic diagram of yield strength as a function of aging time for age-hardenable aluminium alloy[81]

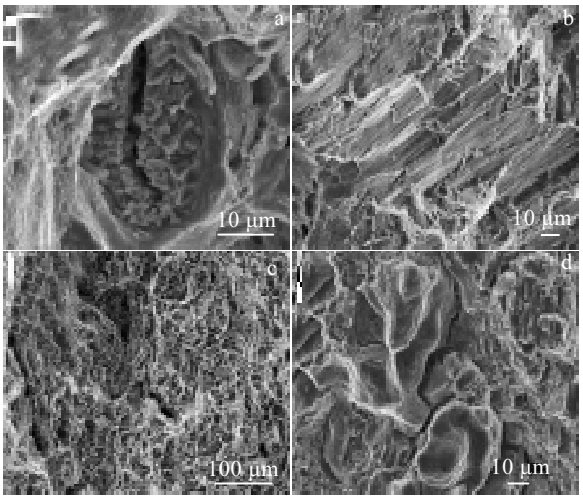

Fig.18 Fracture surfaces of Kahn tear test specimens: (a) intermetallic fracture (intermediate quench), (b) ductile intragranular fracture (fast quench, over-aged), (c) ductile shear fracture (fast quench, under-aged), and (d) intergranular fracture (slow quench, peak-aged)[82]

T74 treatment, and contributes to the secondary age-hardening phenomenon during the cooling procedure. Liu et al[86] found that the nucleating rate increases and the coarsening rate decreases with the appropriate initial aging temperature and cooling rate during the non-isothermal aging treatment. In addition, T6I6 temper was developed by Buha et al[87]. The tensile properties of 7050 alloys after T6I6 temper are similar with those of samples after T6 treatment, but the fracture toughness significantly improves due to the secondary precipitation during the reduced temperature aging stage after under-aging. Stress-aging is an important technique via the mechanical formation and aging treatment. Considerable researches showed that the size and morphology of aging precipitates can be altered by the external stress and stress-aging temperature. For example, Bakavos et al[88] found that the external stress can accelerate the nucleation of GP II zones and the coarsening of stable η phase.

Severe plastic deformation processing is utilized to improve the strength of Al-Zn-Mg-Cu alloys because of the deformation-induced precipitation and segregation of elements at grain boundaries. Recently, Zhang et al[89] found that a controlled cyclic deformation at room temperature is sufficient to continuously inject vacancies into the material and to mediate the dynamic precipitation of solute clusters of 1~2 nm in size, with similar strength but higher elongation, compared to those of alloys after T6 aging temper. The relationship between the multi-scale second phase particles and properties of Al-Zn-Mg-Cu alloy is shown in Fig.19.

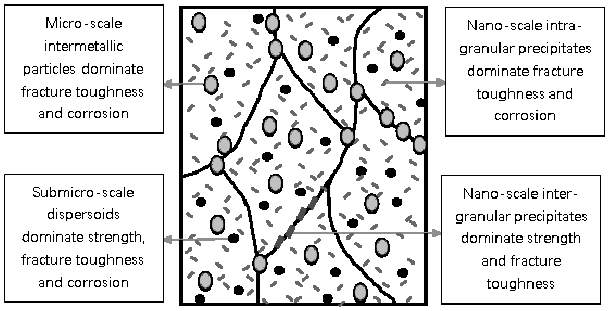

Fig.19 Relationship between multi-scale second phase particles and properties of Al-Zn-Mg-Cu alloys

5 Conclusions

By reviewing the literatures and works of authors in terms of the relationship between multi-scale second phase particles and related properties of Al-Zn-Mg-Cu alloys, some conclusions can be drawn as follows:

1) The micro-scale intermetallic particles dominate corrosion resistance and fracture toughness.

2) Submicro-scale dispersoid inhibits the recrystallization of matrix and dominates the strength, fracture toughness and corrosion resistance.

3) Nano-scale intergranular precipitates dominate the fracture toughness and corrosion resistance.

4) Nano-scale intragranular precipitates dominate the strength and fracture toughness.

References

1 Dursun T, Soutis C. *Materials and Design*[J], 2014, 56: 862
2 Hamerton R G, Cama H, Meredith M W. *Materials Science Forum*[J], 2000, 331-337: 143
3 Andreatta F, Terryn H, De Wit J H W. *Corrosion Science*[J], 2003, 45(8): 1733
4 Jiang F L, Zuros H S, Purdy G R *et al*. *Metallurgical and Materials Transactions A*[J], 2018, 49(10): 5157
5 Hatch J E. *Aluminum: Properties and Physical Metallurgy*[M]. Ohio: American Society for Metals Park, 1984
6 Cvijović Z, Rakin M, Vratnica M *et al*. *Engineering Fracture Mechanics*[J], 2008, 75(8): 2115
7 Vratnica M. *International Journal of Materials Research*[J], 2012, 103(5): 624
8 Birbilis N, Cavanaugh M D, Buchheit R G. *Corrosion Science*[J], 2006, 48(12): 4202
9 Birbilis N, Buchheit R G. *Journal of the Electrochemical Society*[J], 2008, 155(3): 117
10 Wloka J, Börklin G, Virtanen S. *Electrochimica Acta*[J], 2007, 53(4): 2055
11 Bayoumi M R. *Engineering Fracture Mechanics*[J], 1996, 54(6): 879
12 Peng G S, Chen K H, Chen S Y *et al*. *Materials and Corrosion*[J], 2010, 63(3): 254
13 Kannan M B, Raja V S. *Journal of Materials Science*[J], 2007, 42(14): 5458
14 Kamp N, Sinlair I, Starink M J. *Metallurgical and Materials Transactions A*[J], 2002, 33(4): 1125
15 Dong P X, Chen S Y, Chen K H. *Journal of Alloys and Compounds*[J], 2019, 788: 329
16 Mondal C, Mukhopadhyay A K. *Materials Science and Engineering A*[J], 2005, 391(1-2): 367
17 Song M, Chen K H. *Journal of Materials Science*[J], 2008, 43(15): 5265
18 Gao F H, Li N K, Tian N *et al*. *Transactions of Nonferrous Metals Society of China*[J], 2008, 18(2): 321
19 Peng X Y, Li Y, Guo Q *et al*. *JOM*[J], 2018, 70(11): 2692
20 Wang L, Makhlouf M, Apelian D. *International Materials Reviews*[J], 1995, 40(6): 221
21 Sweet L, Easton M A, Taylor J A *et al*. *Metallurgical and Materials Transactions A*[J], 2013, 44(12): 5396
22 Zhang L F, Gao J W, Damoah L N W. *Mineral Processing and Extractive Metallurgy Review*[J], 2012, 33(2): 99
23 Yang W C, Gao F, Ji S X. *Transactions of Nonferrous Metals Society of China*[J], 2015, 25(5): 1704
24 Ji S X, Yang W C, Gao F *et al*. *Materials Science and Engineering A*[J], 2013, 564: 130

25 Nisancioglu K. *Journal of the Electrochemical Society*[J], 1990, 137(1): 69

26 Dorin T, Stanford N, Birbilis N *et al*. *Corrosion Science*[J], 2015, 100: 396

27 Sha G, Wang Y B, Liao X Z *et al*. *Materials Science and Engineering A*[J], 2010, 527(18-19): 4742

28 Morere B, Shahani R, Maurice C *et al*. *Metallurgical and Materials Transactions A*[J], 2001, 32(3): 625

29 Dorward R C, Beerntsen D J. *Metallurgical and Materials Transactions A*[J], 1995, 26(9): 2481

30 Deshpande N U, Gokhale A M, Denzer D K *et al*. *Metallurgical and Materials Transactions A*[J], 1998, 29(4): 1191

31 Fang H C, Chao H, Chen K H. *Journal of Alloys and Compounds*[J], 2015, 622: 166

32 Chen S Y, Chen K H, Dong P X *et al*. *Journal of Alloys and Compounds*[J], 2013, 581: 705

33 Liu S D, Liu W J, Zhang Y *et al*. *Journal of Alloys and Compounds*[J], 2010, 507(1): 53

34 Gronsky R, Furrer P. *Metallurgical Transactions A*[J], 1981, 12(1): 121

35 Li M H, Yang Y Q, Feng Z Q *et al*. *Transactions of Nonferrous Metals Society of China*[J], 2014, 24(7): 2061

36 Minoda T, Yoshida H. *Metallurgical and Materials Transactions A*[J], 2002, 33(9): 2891

37 Kim S H, Erb U, Aust K T. *Scripta Materialia*[J], 2001, 44(5): 835

38 Bechtle S, Kumar M, Somerday B P *et al*. *ActaMaterials*[J], 2009, 57(14): 4148

39 Humphreys F J, Hatherly M. *Recrystallization and Related Annealing Phenomena*[M]. Oxford: Elsevier, 2004: 96

40 Staley J T. *Aluminum Alloys-Contemporary Research and Applications*[M]. Boston: Academic Press, 1989: 17

41 Cassell A M, Robon J D, Race C P *et al*. *Acta Materials*[J], 2019, 169: 135

42 Knipling K E, Dunand D C, Seidman D N. *Acta Materials*[J], 2008, 56(1): 114

43 Seidman D N, Marquis E A, Dunand D C. *Acta Materials*[J], 2002, 50(16): 4021

44 Clouet E, Laé L, Épicier T *et al*. *Nature Materials*[J], 2006, 5(6): 482

45 Robson J D. *Acta Materials*[J], 2004, 52(6): 1409

46 Zhang M, Liu T, He C N *et al*. *Journal of Alloys and Compounds*[J], 2016, 658: 946

47 Buha J. *Acta Materials*[J], 2008, 56(14): 3533

48 Gao T, Zhang Y R, Liu X F. *Materials Science and Engineering A*[J], 2014, 598: 293

49 Peng G S, Chen K H, Fang H C *et al*. *Materials and Design*[J], 2012, 36: 279

50 Peng G S, Chen K H, Fang H C. *Materials Science and Engineering A*[J], 2012, 535: 311

51 Fang H C, Chen K H, Zhang Z *et al*. *Transactions of Nonferrous Metals Society of China*[J], 2008, 18(1): 28

52 Karnesky R A, Dunand D C, Seidman D N. *Acta Materials*[J], 2009, 57(14): 4022

53 Robson J D, Prangnell P B. *Acta Materials*[J], 2001, 49(4): 599

54 Robson J D. *Materials Science and Engineering A*[J], 2002, 338(1-2): 219

55 Deng Y L, Zhang Y Y, Wan L *et al*. *Metallurgical and Materials Transactions A*[J], 2013, 44(6): 2470

56 Peng G S, Chen K H, Chen S Y *et al*. *Materials and Corrosion*[J], 2012, 63(3): 254

57 Peng G S, Chen K H, Chen S Y. *Materials Science and Engineering A*[J], 2015, 641: 237

58 Ran F Q, Chai L H, Gao K Y *et al*. *Corrosion Engineering Science and Technoloogy*[J], 2014, 49(8): 712

59 Liu S D, Chen B, Li C B *et al*. *Corrosion Science*[J], 2015, 91: 203

60 Knight S P, Pohl K, Holroyd N J H *et al*. *Corrosion Science*[J], 2015, 98: 50

61 Song R G, Tseng M K, Zhang B J *et al*. *Acta Materials*[J], 1996, 44(8): 3241

62 Marlaud T, Deschamps A, Bley F *et al*. *Acta Materials*[J], 2010, 58(1): 248

63 Zhao H, Geuser F D, Silva A K D *et al*. *Acta Materials*[J], 2018, 156: 318

64 Robson J D. *Materials Characterization*[J], 2019, 154: 325

65 Li D F, Yin B W, Lei Y *et al*. *Metals and Materials International*[J], 2016, 22(2): 222

66 Azarniya A, Taheri A K, Taheri K K. *Journal of Alloys and Compounds*[J], 2019, 781: 945

67 Shreir L L. *Corrosion*[M]. London: Newnes, 1976, 1: 49

68 Feng C, Liu Z Y, Ning A L *et al*. *Transactions of Nonferrous Metals Society of China*[J], 2006, 16(5): 163

69 Peng G S, Chen K H, Chen S Y *et al*. *Materials Science and Engineering A*[J], 2011, 528(12): 4014

70 Liu Y, Jiang D M, Li W J *et al*. *Journal of Alloys and Compounds*[J], 2016, 671: 408

71 Yang J G, Ou B L. *Scandinavian Journal of Metallurgy*[J], 2001, 30(3): 158

72 Yuan D L, Chen K H, Chen S Y *et al*. *Materials and Design*[J], 2019, 164: 107 558

73 Huang L P, Chen K H, Li S *et al*. *Scripta Materialia*[J], 2007, 56(4): 305

74 Huang L P, Chen K H, Li S. *Materials Science and Engineering B*[J], 2012, 177(11): 862

75 Wang D, Ma Z Y, Gao Z M. *Materials Chemistry and Physics*[J], 2009, 177(1): 228

76 Sha G, Cerezo A. *Acta Materials*[J], 2004, 52(15): 4503

77 Fan X G, Jiang D M, Meng Q C *et al*. *Materials Science and Engineering A*[J], 2006, 427(1-2): 130

78 Deschamps A, Brechet Y. *Materials Science and Engineering A*[J], 1998, 251(1-2): 200

79 Chen J Z, Zhen L, Yang S J *et al*. *Materials Science and Engineering A*[J], 2009, 500(1-2): 34

80 Staley L T. *Microstructure and Toughness of High Strength Alloys*[M]. Pennsylvania: ASTM International, 1975
81 Roger L. *Fundamentals of Aluminium Metallurgy: Production, Processing and Applications*[M]. Oxford: Woodhead Publishing, 2011: 131
82 Dumont D, Deschamps A, Brechet Y. *Acta Materials*[J], 2004, 52(9): 2529
83 Zhu Q Q, Gao L F, Wu X D *et al*. *Materials Science and Engineering A*[J], 2019, 754: 265
84 Lim S T, Yun S J, Nam S W. *Materials Science and Engineering A*[J], 2004, 371(1-2): 82
85 Jiang D M, Liu Y, Liang S *et al*. *Journal of Alloys and Compounds*[J], 2016, 681: 57
86 Liu Y, Jiang D M, Li B Q *et al*. *Materials and Design*[J], 2014, 57: 79
87 Buha J, Lumley R N, Crosky A G. *Materials Science and Engineering A*[J], 2008, 492(1-2): 1
88 Bakavos D, Prangnell P B, Bès B *et al*. *Materials Science Forum*[J], 2006, 519-521: 333
89 Zhang Y D, Jin S B, Trimby P W *et al*. *Acta Materials*[J], 2019, 162: 19

Al-Zn-Mg-Cu 合金多尺度第二相粒子与性能关系研究

彭国胜[1]，顾亦诚[1]，陈送义[2]，陈康华[2]，方华婵[3]，宋广生[1]

(1. 安徽工业大学 材料科学与工程学院 先进金属材料绿色制备与表面技术教育部重点实验室，安徽 马鞍山 243002)

(2. 中南大学 高性能复杂制备国家重点实验室，湖南 长沙 410083)

(3. 中南大学 粉末冶金国家重点实验室，湖南 长沙 410083)

摘　要：介绍了 Al-Zn-Mg-Cu 合金多尺度第二相粒子与性能关系的研究。涉及的多尺度第二相粒子包括微米尺度的金属间化合物、亚微米尺度的弥散相、纳米尺度的晶内析出相和晶界析出相；涉及的相关性能为强度、断裂韧性以及腐蚀性能。结合相关文献与作者的研究工作，可以得出以下结论：金属间化合物会影响合金的断裂韧性和腐蚀抗力；弥散相通过抑制基体再结晶的方式影响合金的强度、断裂韧性以及腐蚀抗力；晶界析出相会影响合金的断裂韧性和腐蚀抗力；晶内析出相影响合金的强度和断裂韧性。

关键词：Al-Zn-Mg-Cu合金；金属间化合物；弥散相；析出相；性能

作者简介：彭国胜，男，1978 年生，博士，副教授，安徽工业大学材料科学与工程学院，安徽 马鞍山 243002，电话：0555-2311570，E-mail: pengguosheng@126.com